



Computational Exploration of Intrinsic Rashba Splitting in Janus Si₂SbBi Monolayer Using Density Functional Theory

Yusuf Affandi^{1a}, Yusron Darajat², Muhammad Anshory², and Awi Masfufah³

1. Instrumentation and Automation Engineering, Faculty of Industrial Technology, Institut Teknologi Sumatera, Lampung Selatan, Indonesia, 35365
2. Department of Physics, Faculty of Science, Institut Teknologi Sumatera, Lampung Selatan, Indonesia, 35365
3. Bachelor Program of Instrumentation and Automation Engineering, Faculty of Industrial Technology, Institut Teknologi Sumatera, Lampung Selatan, Indonesia, 35365

Article Information

Article history:

Received January 22, 2024

Received in revised form
January 25, 2024

Accepted January 26, 2024

Keywords: DFT, Electronic Structure, Janus, Rashba Splitting, Spintronics

Abstract

In this paper, we investigate the electronic structure of Janus Si₂SbBi monolayer and compare it with the non-polar systems Si₂Bi₂ and Si₂Sb₂ monolayer based on Density Functional Theory (DFT) calculation. According to the first-principles calculation, these systems exhibit semiconductor properties with energy gaps are 0.674 eV, 0.28 eV, and 1.13 eV for Janus Si₂SbBi, Si₂Bi₂, and Si₂Sb₂, respectively. In addition, the intrinsic Rashba splitting is also observed around the Γ Point on conduction band minimum (CBM) in the electronic structure of Si₂SbBi monolayer, which is not found in Si₂Sb₂ and Si₂Bi₂ monolayer systems. This Rashba splitting phenomenon we analyze by using the $k \cdot p$ perturbation theory based on symmetry group and get the first-order Rashba Parameter $\alpha_1 = 1.84 \text{ eV}\text{\AA}$, and $\alpha_1 = 1.73 \text{ eV}\text{\AA}$, for Γ -K and Γ -M direction, respectively. Given its robust intrinsic Rashba Splitting, the Janus Si₂SbBi monolayer exhibits promising potential as a semiconductor material for spintronics devices.

Informasi Artikel

Proses artikel:

Diterima 22 Januari 2024

Diterima dan direvisi dari
25 Januari 2024

Accepted 26 Januari 2024

Kata kunci: DFT, Janus, Rashba Splitting, Struktur Elektronik, Spintronics

Abstrak

Penelitian ini kami menginvestigasi struktur elektronik dari material Janus Si₂SbBi monolayer dan membandingkannya dengan material non-polar Si₂Sb₂ dan Si₂Bi₂ monolayer berbasis perhitungan Density Functional Theory (DFT). Berdasarkan perhitungan first-principles semua sistem menunjukkan sifat semikonduktor dengan energi gap yaitu 0.674 eV, 0.28 eV, dan 1.13 eV untuk masing-masing dari material Si₂SbBi, Si₂Bi₂, dan Si₂Sb₂ monolayer. Selain itu instrinsik Rashba Splitting juga teramati di sekitar Γ point pada conduction band minimum (CBM) di struktur elektronik dari Si₂SbBi monolayer yang tidak ditemukan pada material Si₂Bi₂, dan Si₂Sb₂ monolayer. Fenomena Rashba splitting tersebut kami analisis menggunakan teori gangguan $k \cdot p$ yang dikombinasikan dengan symmetry group dan memperoleh parameter Rashba order pertama $\alpha_1 = 1.84 \text{ eV}\text{\AA}$, dan $\alpha_1 = 1.73 \text{ eV}\text{\AA}$, untuk masing-masing arah Γ -K point dan arah Γ -M point. Sifat instrinsik Rashba splitting yang kuat membuat material Janus Si₂SbBi monolayer memiliki potensi yang baik sebagai kandidat material semikonduktor untuk divais spintronics.

1. Introduction

In recent years, research on two-dimensional materials has been widely studied by researchers after discovering graphene as a pioneering two-dimensional material due to its outstanding electronic and spintronic properties (Hanna et al., 2018; Lee et al., 2017). However, graphene has a small energy bandgap and weak spin-orbit

* Corresponding author.

E-mail address: yusuf.affandi@ia.itera.ac.id

interaction (SOI), so it cannot be used for semiconductor applications. As a result, research to find new two-dimensional materials having hexagonal structures, such as graphene with semiconductor properties, has attracted much attention from researchers ever since. These new materials are including MXenes (Huang et al., 2020; Nan et al., 2021), hexagonal Boron nitride (Garcia-Miranda Ferrari et al., 2021; K. Zhang et al., 2017), transition metal dichalcogenides (TMDs) (Affandi et al., 2018; Affandi & Ulil Absor, 2019), Janus transition metal dichalcogenides (Janus TMDs) (Putri et al., 2021; Sino et al., 2021) and monolayer IV-V materials (Morales-Ferreiro et al., 2017).

Materials with strong SOI are particularly interesting because they lead to various phenomena such as spin Hall effect (Bandurin et al., 2017; Qi et al., 2006), Zeeman effect (Wang et al., 2020), Topological Insulator (Huang et al., 2020), and Rashba effect (Bychkov & Rashba, 1984). In particular, Rashba effect attracts much attention due to its potential in spintronic devices like spin field effect transistor (sFET). The Rashba effect is a momentum-dependent spin splitting in materials with a non-centrosymmetry structure (Affandi & Ulil Absor, 2019; Putri et al., 2021). Experimentally, Rashba effect is observed in AlGaAs/GaAs by magnetotransport measurements (Stein et al., 1983). In a theoretical study, Rashba effect predicted appears in many 2D materials such as in heavy metal film (Mihai Miron et al., 2010), in TMDs (Affandi & Ulil Absor, 2019), and Janus TMDs (Putri et al., 2021). Interestingly, Rashba effect is tunable by some external effects such as by external electric field (Affandi & Ulil Absor, 2019) and by strain engineering effect (Anshory & Absor, 2020; Putri et al., 2021).

The Rashba effect is indicated by the significant spin splitting in the electronic structure of materials around the Fermi level, which is referred to as Rashba Spin Splitting (RSS). Intrinsic RSS has been reported to appear in Janus TMDs due to breaking inversion symmetry in the crystal structure (Putri et al., 2021; Sino et al., 2021). Similar to Janus TMDs, the RSS is predicted to emerge in Janus material from the monolayer IV-V family. Monolayer IV-V materials are defined by a general formula A_2X_2 with A corresponding to the group IV atoms and X corresponding to the group V atom. Recently, A_2X_2 single-layer structure and novel electronic properties have been synthesized (W. Zhang et al., 2018). On the other hand, Janus IV-V ML materials are derived from the original IV-V ML with the chemical formula of A_2XY , where one of the V atom (X) replaced by a different atom of group V (Y).

Among the Janus IV-V ML materials, the Janus Si_2SbBi ML predicted have strong RSS due to strong SOI of Sb and Bi atoms. Therefore, in this study, by Density Functional Theory (DFT) calculations, we identified the electronic structure of the Janus material Si_2SbBi ML and the original structure Si_2X_2 ML for comparison. We also analyze the intrinsic RSS on Janus material Si_2SbBi ML by using $k \cdot p$ perturbation theory combined with the symmetry group. Finally, the possible applications of the present systems for spintronics are discussed.

2. Research Methods

In this study, we employed Density Functional Theory (DFT) calculations using the OpenMX software package (Ozaki et al., 2009) to carry out the electronic structure of the material. The exchange-correlation functional employed in this study was the Generalized Gradient Approximation by Perdew, Burke, and Ernzerhof (GGA-PBE) (Perdew et al., 1996). The norm-conserving pseudopotential (Troullier & Martins, 1991) is applied in our calculation with an energy cutoff 300 Ry for charge density. We utilized a linear combination of multiple pseudoatomic orbitals to extend the wavefunction by using a confinement scheme (Ozaki, 2003; Ozaki & Kino, 2004). In this approach, two s -, two p -, and one d -character numerical pseudo-atomic orbitals were used for each atom. Additionally, our fully relativistic calculations incorporated the Spin-Orbit Interaction (SOI) (Theurich & Hill, 2001).

In our computational simulations, we represent the two-dimensional configuration of Janus Si_2SbBi and Si_2X_2 ($\text{X}=\text{Sb}, \text{Bi}$) through a periodic slab, ensuring a substantial 24 Å vacuum layer to prevent interactions between adjacent layers. Employing a $12 \times 12 \times 1$ k -point grid, we conducted a thorough relaxation of atomic positions, adhering to a stringent force criterion of 1×10^{-5} Hartree/Bohr to achieve optimized geometries.

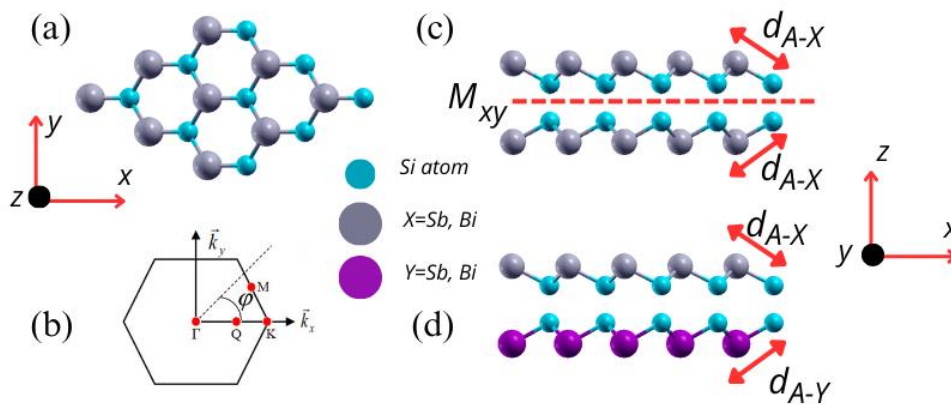


Figure 1. (a) Top view of both Si_2X_2 ($\text{X}=\text{Sb}, \text{Bi}$) ML and Janus Si_2SbBi ML. (b) The first Brillouin zone of both Si_2X_2 ($\text{X}=\text{Sb}, \text{Bi}$) and Janus Si_2SbBi ML. (c) Side view of Si_2X_2 ($\text{X}=\text{Sb}, \text{Bi}$) ML and (d) Janus Si_2SbBi ML and presenting bond length between atom Si with X (Sb, Bi) atom (d_{A-X}), and between atom Si with Y (Sb, Bi, $\text{X} \neq \text{Y}$) atom (d_{A-Y}).

The crystal structure of Si_2X_2 ($\text{X}=\text{Sb}, \text{Bi}$) is formed by group IV-V compounds with an A_2X_2 ML structure can be seen in **Figure 1**. (a) Top view of both Si_2X_2 ($\text{X}=\text{Sb}, \text{Bi}$) ML and Janus Si_2SbBi ML. (b) The first Brillouin zone of both Si_2X_2 ($\text{X}=\text{Sb}, \text{Bi}$) and Janus Si_2SbBi ML. (c) Side view of Si_2X_2 ($\text{X}=\text{Sb}, \text{Bi}$) ML and (d) Janus Si_2SbBi ML and presenting bond length between atom Si with X (Sb, Bi) atom (d_{A-X}), and between atom Si with Y (Sb, Bi, $\text{X} \neq \text{Y}$) atom (d_{A-Y}). These compounds consist of quadruple atomic layers held together by covalent bonds and organized in a repeating sequence of $\text{X}-\text{A}-\text{A}-\text{X}$. These arrangement makes A_2X_2 ML possess crystal symmetry corresponding to the P6m2 space

group with a D_{3h} point group. On the other hand, the crystal structure of Janus Si_2SbBi ML is transformed from A_2X_2 ML structure, which is formed by replacing group V atom on one side with a different group V atom, resulting a broken mirror symmetry. Consequently, the Janus Si_2SbBi ML has crystal symmetry with C_{3v} point group.

3. Results and Discussions

Table 1. Optimized structural parameters of Janus Si_2SbBi ML and non-Janus Si_2X_2 ($\text{X}=\text{Sb}, \text{Bi}$) ML for comparative analysis. Includes in-plane lattice constants a , the bond length between A and X (d_{A-X}), and the bond length between A and Y (d_{A-Y}).

Systems	a (Å)	d_{A-X} (Å)	d_{A-Y} (Å)	E_{gap} (eV)	Ref
Si_2SbBi ML	4.010	2.668	2.715	0.674	This work
Si_2Sb_2 ML	4.000	2.633	-	1.13	This work
Si_2Bi_2 ML	4.128	2.724	-	0.28	This work

Initially, we examine the structural parameters of the Janus Si_2SbBi ML, as detailed in **Table 1**. Our analysis reveals an optimized in-plane lattice constant of 4.01 Å, in line with previously reported calculations (Babaei Touski & Ghobadi, 2021; Lukmantoro & Absor, 2023). For comparison, we also conducted calculations for non-Janus Si_2X_2 ($\text{X}=\text{Sb}, \text{Bi}$) ML and we found the lattice constant are 4.000 Å and 4.128 Å for Si_2Sb_2 and Si_2Bi_2 ML, respectively. These findings indicate that the lattice constant of the Janus Si_2SbBi ML falls approximately midway between those of Si_2Sb_2 and Si_2Bi_2 MLs.

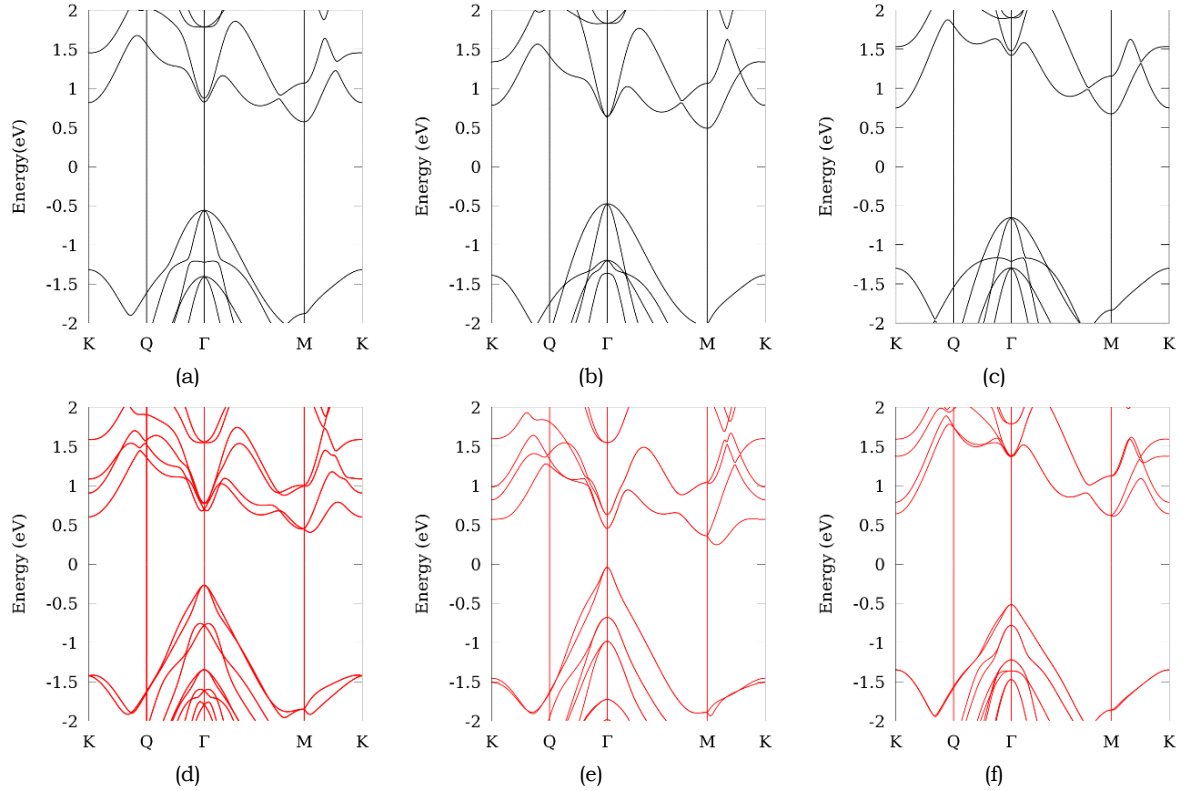


Figure 2. Electronic structures of Janus Si_2SbBi ML, Si_2Bi_2 ML, and Si_2Sb_2 ML, without (a-c) and with (d-f) consideration of Spin Orbit Interaction (SOI), respectively.

Figure 2. Electronic structures of Janus Si_2SbBi ML, Si_2Bi_2 ML, and Si_2Sb_2 ML, without (a-c) and with (d-f) consideration of Spin Orbit Interaction (SOI), respectively. illustrates the electronic structure of the Janus Si_2SbBi ML in comparison to non-Janus Si_2X_2 ($\text{X}=\text{Sb}, \text{Bi}$) MLs. The calculations were performed both without (a-c) and with (d-f) consideration of the SOI. All systems exhibit an indirect band gap, where conduction band minimum (CBM) and valence band maximum (VBM) are located at the M and Γ points, respectively. The inclusion of SOI influences the energy gap in all systems, leading to a reduction in the energy gap when compared to calculations without SOI. The Janus Si_2SbBi ML has an energy gap of 0.674 eV, which is smaller than Si_2Sb_2 ML 1.13 eV, but slightly larger than Si_2Bi_2 ML 0.28 eV. Detailed calculation results are provided in **Table 1**.

Our attention is directed towards the Janus Si_2SbBi ML with Spin-Orbit Interaction (SOI). Notably, the Rashba spin splitting (RSS) effect manifests in the conduction band near the Γ point (**Figure 3**.(a)), a phenomenon absent in the non-Janus Si_2X_2 ML system. This occurrence is attributed to the broken mirror symmetry within the Janus Si_2SbBi ML system. Analysis of the band projections onto the atoms confirms that the Rashba-type spin splitting around Γ point arises from significant interactions among Bi- $(px+py)$, Bi- (pz) , Sb- $(px+py)$, and Sb- pz orbitals (**Figure 3**.(b)). The observed spin splitting around Γ point in the Janus Si_2SbBi ML is expected to play a crucial role in creating spin-polarized states via the Rashba effect. This has notable implications for the functionality of spin-field effect transistors.

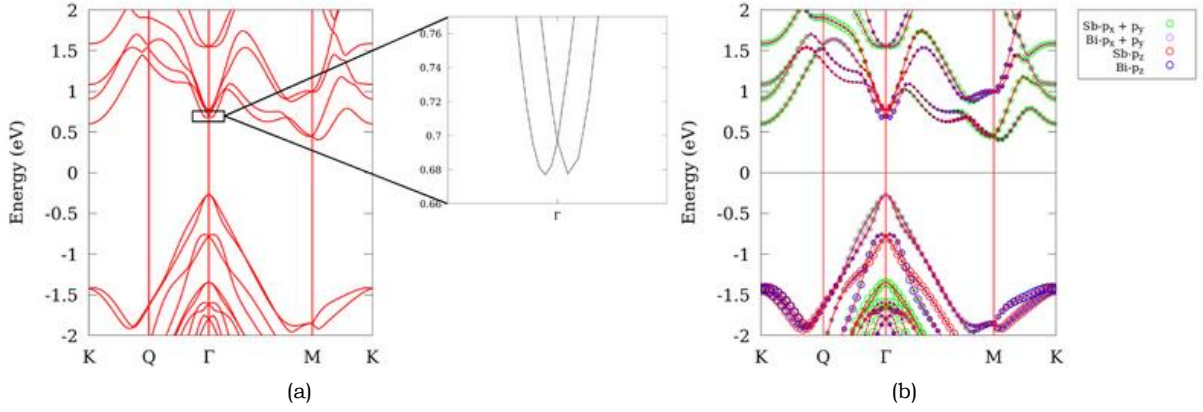


Figure 3. The electronic structure of the Janus Si₂SbBi ML system, highlighting the Rashba spin splitting (RSS) with a black rectangle around the Γ point in the magnified view **(a)**. The projected orbital band of the Janus Si₂SbBi ML, featuring colored contributions and spectral weights represented by circle radius **(b)**.

To analyze the RSS, first, we can consider that this system is like a 2-dimensional electron gas (2DEG) system. In a 2DEG system, the energy of RSS can be written as follows Eq. (1).

$$E^{\pm}(\vec{k}) = \frac{\hbar^2 \vec{k}^2}{2m^*} \pm \alpha_R |\vec{k}| \quad (1)$$

where $E^{\pm}(\vec{k})$ is the energy band of spin up and down as wave vector k function, \hbar is Plank's constant, m^* is electron mass, and α_R is Rashba parameter. Based on this equation, the Rashba parameter α_R equation can be written as Eq (2).

$$\alpha_R = \frac{2\Delta E_R}{\Delta k} \quad (2)$$

Based on this equation, we found that Rashba parameter α_R of 3.55 eVÅ (see **Table 2**).

The another way to analyze the RSS, we can use the $k \cdot p$ perturbation theory based on symmetry group (Vajna et al., 2012). The Janus Si₂SbBi ML has crystal symmetry with C_{3v} point group. The effective Hamiltonian at the Γ point can be expressed as Eq (3).

$$H_R(k) = E_0(k) + \alpha(k)[\cos(\phi)\sigma_y - \sin(\phi)\sigma_x] + \alpha_3^2 k^3 \cos(3\phi)\sigma_z \quad (3)$$

where $E_0(k) = \frac{\hbar^2 k^2}{2m^*}$ and m^* is the effective mass, $\alpha(k) = \alpha_1 k + \alpha_3^1$, with α_1 and α_3^1 are the first and third orders Rashba parameters, respectively, while α_3^2 is the warping parameter. In addition, we define a polar angle, ϕ , in k -space through the relation $\phi = \cos^{-1}(\frac{k_x}{k})$. Solving eigenvalue problem associated with the Hamiltonian, we derive the spin splitting energy expressed in the square form in Eq (4).

$$[\Delta E(k)]^2 = (\alpha_1 k + \alpha_3^1 k^3)^2 + (\alpha_3^2)^2 k^6 \cos^2 3\phi \quad (4)$$

For direction of Γ -K point and Γ -M point, the polar angle are $\phi = (0^\circ, 60^\circ \dots)$ and $\phi = (30^\circ, 90^\circ, \dots)$, respectively.

Table 2 shows the Rashba parameter result from fitting calculation with Equation 4 for small value of k . For Γ -K direction, our fitting calculation, found that $\alpha_1 = 1.84$ eVÅ and $\alpha_3^1 = -337.95$ eVÅ³ and $\alpha_3^2 = -236.86$ eVÅ³. However, for Γ -M direction our fitting calculation, found that $\alpha_1 = 1.73$ eVÅ and $\alpha_3^1 = -227.35$ eVÅ³. The calculated value of the first order Rashba parameter α_1 for both directions is closely matches the Rashba parameter α_R derived for the 2DEG equation. This similarity indicates that RSS in the Janus Si₂SbBi ML system is isotropic, which is further supported by the relatively small third-order Rashba parameter obtained from the fitting calculation.

Table 2. The Rashba parameter result derived from Equation 2 and fitting calculation with Eq (4).

System	α_R (eVÅ)	Γ -K			Γ -M	
		α_1 (eVÅ)	α_3^1 (eVÅ ³)	α_3^2 (eVÅ ³)	α_1 (eVÅ)	α_3^1 (eVÅ ³)
Janus Si ₂ SbBi ML	1.88	1.84	-337.95	-236.86	1.73	-227.35

In order to validate the existence of Rashba splitting, we conducted spin polarization calculations specifically around the Γ point at the conduction band minimum (CBM). Our analysis involved spin texture calculations, where we plotted the expectation value of spin in the x, y, and z directions. As depicted in **Figure 4**, the spin textures of the Janus Si₂SbBi ML around the Γ point unequivocally affirm the presence of the Rashba effect in this system. The spin

textures have a circular pattern with two components of spins consist of the clock wise and the counter clock wise one direction. This pattern implies and confirm that the Rashba effect characteristic of the system tend to be isotropic.

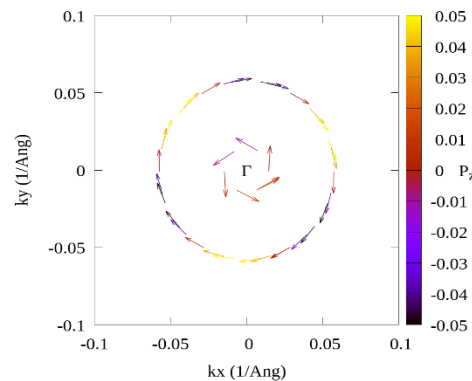


Figure 4. Spin texture of the Janus Si₂SbBi ML system around the Γ point in the CBM for small of k .

We observed that the presence of Rashba spin splitting (RSS) in the Janus Si₂SbBi ML system could be experimentally verified (Rezavand et al., 2022), similar to how the spin splitting in the MoS₂ monolayer has been observed in experiments (Jin et al., 2015). Given its substantial Rashba parameter, this system holds potential for future applications in spin field-effect transistor (SFET) devices. Consequently, we anticipate that our findings will instigate further theoretical and experimental endeavors to explore the Rashba effect in the Janus Si₂SbBi ML system, thereby broadening the range of 2D materials suitable for prospective applications in spintronics.

4. Conclusion

In conclusion, our investigation delved into the existence of Rashba splitting properties in the Janus Si₂SbBi monolayer (ML) system through first-principles Density Functional Theory (DFT) calculations. The findings revealed a substantial Rashba splitting around the Γ point in the Conduction Band Minimum (CBM) with an isotropic character. The Rashba parameter was comprehensively explained and analyzed using $k \cdot p$ perturbation theory based on symmetry group, drawing comparisons with the isotropic equation for Rashba in a two-dimensional electron gas (2DEG). The isotropic characteristic of the Rashba parameter is contributed by the first order Rashba parameter, and negative contributed by third order Rashba parameter. Therefore, our results provide the Janus Si₂SbBi ML system is well-suited as a potential candidate for spintronic materials in Spin Field-Effect Transistor (SFET) devices.

5. Bibliography

- Affandi, Y., Absor, M. A. U., & Abraha, K. (2018). Effect of external electric field on spin-orbit splitting of the two-dimensional tungsten dichalcogenides WX₂ (X = S, Se). *Journal of Physics: Conference Series*, 1011(1). <https://doi.org/10.1088/1742-6596/1011/1/012070>
- Affandi, Y., & Ulil Absor, M. A. (2019). Electric field-induced anisotropic Rashba splitting in two dimensional tungsten dichalcogenides WX₂ (X: S, Se, Te): A first-principles study. *Physica E: Low-Dimensional Systems and Nanostructures*, 114(March), 1–6. <https://doi.org/10.1016/j.physe.2019.113611>
- Anshory, M., & Absor, M. A. U. (2020). Strain-controlled spin-splitting in the persistent spin helix state of two-dimensional SnSe monolayer. *Physica E: Low-Dimensional Systems and Nanostructures*, 124(May), 114372. <https://doi.org/10.1016/j.physe.2020.114372>
- Babaei Touski, S., & Ghobadi, N. (2021). Structural, electrical, and Rashba properties of monolayer Janus Si₂XY (X,Y =P, As, Sb, and Bi). *Physical Review B*, 103(16). <https://doi.org/10.1103/PhysRevB.103.165404>
- Bandurin, D. A., Tyurnina, A. V., Mishchenko, A., Zolyomi, V., Morozov, S. V., Krishna Kumar, R., Gorbachev, R. V., Kudrynskiy, Z. R., Pezzini, S., Kovalyuk, Z. D., Zeitler, U., Novoselov, K. S., Patenè, A., Eaves, L., Grigorieva, I. V., Fal'ko, V. I., Geim, A. K., & Cao, Y. (2017). Mobility, High Electron Effect, Quantum Hall Response, Anomalous Optical Thin, Atomically InSe. *Nature Nanotechnology*, 12(3), 1–18.
- Bychkov, Y. A., & Rashba, E. I. (1984). Properties of a 2D electron gas with lifted spectral degeneracy. In *JETP Letters* (Vol. 39, pp. 78–81).
- García-Miranda Ferrari, A., Rowley-Neale, S. J., & Banks, C. E. (2021). Recent advances in 2D hexagonal boron nitride (2D-hBN) applied as the basis of electrochemical sensing platforms. *Analytical and Bioanalytical Chemistry*, 413(3), 663–672. <https://doi.org/10.1007/s00216-020-03068-8>
- Hanna, M. Y., Santoso, I., & Ulil Absor, M. A. (2018). The Role of the Oxygen Impurity on the Electronic Properties of Monolayer Graphene: A Density-Functional Study. *Journal of Physics: Conference Series*, 1011(1). <https://doi.org/10.1088/1742-6596/1011/1/012071>

-
- Huang, Z.-Q., Xu, M.-L., Macam, G., Hsu, C.-H., & Chuang, F.-C. (2020). Large-gap topological insulators in functionalized ordered double transition metal carbide MXenes. *Phys. Rev. B*, 102(7), 75306. <https://doi.org/10.1103/PhysRevB.102.075306>
- Jin, W., Yeh, P. C., Zaki, N., Zhang, D., Liou, J. T., Sadowski, J. T., Barinov, A., Yablonskikh, M., Dadap, J. I., Sutter, P., Herman, I. P., & Osgood, R. M. (2015). Substrate interactions with suspended and supported monolayer MoS₂: Angle-resolved photoemission spectroscopy. *Physical Review B - Condensed Matter and Materials Physics*, 91(12). <https://doi.org/10.1103/PhysRevB.91.121409>
- Lee, H. C., Liu, W. W., Chai, S. P., Mohamed, A. R., Aziz, A., Khe, C. S., Hidayah, N. M. S., & Hashim, U. (2017). Review of the synthesis, transfer, characterization and growth mechanisms of single and multilayer graphene. *RSC Advances*, 7(26), 15644–15693. <https://doi.org/10.1039/C7RA00392G>
- Lukmantoro, A., & Absor, M. A. U. (2023). *Anisotropic Rashba splitting dominated by out-of-plane spin polarization in two-dimensional Janus XA₂Y (A= Si, Sn, Ge; X,Y= Sb, Bi) with surface imperfection*. 1–28. <http://arxiv.org/abs/2308.06761>
- Mihai Miron, I., Gaudin, G., Auffret, S., Rodmacq, B., Schuhl, A., Pizzini, S., Vogel, J., & Gambardella, P. (2010). Current-driven spin torque induced by the Rashba effect in a ferromagnetic metal layer. *Nature Materials*, 9(3), 230–234. <https://doi.org/10.1038/nmat2613>
- Morales-Ferreiro, J. O., Diaz-Droguett, D. E., Celentano, D., & Luo, T. (2017). First-Principles Calculations of Thermoelectric Properties of IV–VI Chalcogenides 2D Materials. *Frontiers in Mechanical Engineering*, 3(December), 1–10. <https://doi.org/10.3389/fmech.2017.00015>
- Nan, J., Guo, X., Xiao, J., Li, X., Chen, W., Wu, W., Liu, H., Wang, Y., Wu, M., & Wang, G. (2021). Nanoengineering of 2D MXene-Based Materials for Energy Storage Applications. *Small*, 17(9), 1902085. <https://doi.org/https://doi.org/10.1002/sml.201902085>
- Ozaki, T. (2003). Variationally optimized atomic orbitals for large-scale electronic structures. *Phys. Rev. B*, 67(15), 155108. <https://doi.org/10.1103/PhysRevB.67.155108>
- Ozaki, T., & Kino, H. (2004). Numerical atomic basis orbitals from H to Kr. *Phys. Rev. B*, 69(19), 195113. <https://doi.org/10.1103/PhysRevB.69.195113>
- Ozaki, T., Kino, H., Yu, J., Han, M. J., Kobayashi, N., Ohfuti, M., Ishii, F., Ohwaki, T., Weng, H., & Terakura, K. (2009). OpenMX: Open source package for Material eXplorer. URL: *Www. Openmx-Square. Org*.
- Perdew, J. P., Burke, K., & Ernzerhof, M. (1996). Generalized gradient approximation made simple. *Physical Review Letters*, 77(18), 3865–3868. <https://doi.org/10.1103/PhysRevLett.77.3865>
- Putri, S. A., Suharyadi, E., & Absor, M. A. U. (2021). Polarity effect on the electronic structure of molybdenum dichalcogenides moxy (X, Y = S, Se): A computational study based on density-functional theory. *Indonesian Journal of Chemistry*, 21(3), 598–608. <https://doi.org/10.22146/ijc.57949>
- Qi, X.-L., Wu, Y.-S., & Zhang, S.-C. (2006). Topological quantization of the spin Hall effect in two-dimensional paramagnetic semiconductors. *Physical Review B*, 74(8), 085308. <https://doi.org/10.1103/PhysRevB.74.085308>
- Rezavand, A., Ghobadi, N., & Behnamghader, B. (2022). MSi₂PxAsy (M = Mo, W) monolayers. *Phys. Rev. B*, 106(3), 35417. <https://doi.org/10.1103/PhysRevB.106.035417>
- Sino, P. A. L., Feng, L. Y., Villaos, R. A. B., Cruzado, H. N., Huang, Z. Q., Hsu, C. H., & Chuang, F. C. (2021). Anisotropic Rashba splitting in Pt-based Janus monolayers PtXY (X,Y = S, Se, or Te). *Nanoscale Advances*, 3(23), 6608–6616. <https://doi.org/10.1039/d1na00334h>
- Stein, D., Klitzing, K. v., & Weimann, G. (1983). Electron Spin Resonance on GaAs-AlxGa1-xAs Heterostructures. *Phys. Rev. Lett.*, 51(2), 130–133. <https://doi.org/10.1103/PhysRevLett.51.130>
- Theurich, G., & Hill, N. A. (2001). Self-consistent treatment of spin-orbit coupling in solids using relativistic fully separable ab initio pseudopotentials. *Phys. Rev. B*, 64(7), 73106. <https://doi.org/10.1103/PhysRevB.64.073106>
- Troullier, N., & Martins, J. L. (1991). Efficient pseudopotentials for plane-wave calculations. *Phys. Rev. B*, 43(3), 1993–2006. <https://doi.org/10.1103/PhysRevB.43.1993>
- Vajna, S., Simon, E., Szilva, A., Palotas, K., Ujfalussy, B., & Szunyogh, L. (2012). Higher-order contributions to the Rashba-Bychkov effect with application to the Bi/Ag(111) surface alloy. *Physical Review B - Condensed*

Matter and Materials Physics, 85(7), 1–7. <https://doi.org/10.1103/PhysRevB.85.075404>

Wang, T., Miao, S., Li, Z., Meng, Y., Lu, Z., Lian, Z., Blei, M., Taniguchi, T., Watanabe, K., Tongay, S., Smirnov, D., & Shi, S.-F. (2020). Giant Valley-Zeeman Splitting from Spin-Singlet and Spin-Triplet Interlayer Excitons in WSe₂/MoSe₂ Heterostructure. *Nano Letters*, 20(1), 694–700. <https://doi.org/10.1021/acs.nanolett.9b04528>

Zhang, K., Feng, Y., Wang, F., Yang, Z., & Wang, J. (2017). Two dimensional hexagonal boron nitride (2D-hBN): synthesis, properties and applications. *J. Mater. Chem. C*, 5(46), 11992–12022. <https://doi.org/10.1039/C7TC04300G>

Zhang, W., Yin, J., Ding, Y., Jiang, Y., & Zhang, P. (2018). Strain-engineering tunable electron mobility of monolayer IV–V group compounds. *Nanoscale*, 10(35), 16750–16758. <https://doi.org/10.1039/C8NR04186E>